An AI-Assisted Drone Survey for Mojave Desert Tortoises within the Boulder City Conservation Easement, Clark County, NV

Report submitted to
Desert Conservation Program
Clark County

Matthew Bandy
Resi Solutions

Resi-2024-015-01
July 2024

An AI-Assisted Drone Survey for Mojave Desert Tortoises within the Boulder City Conservation Easement, Clark County, NV

Report submitted to Clark County Desert Conservation Program

Matthew Bandy

July, 2024

Resi-2024-015-01

Resi Solutions

Executive Summary

This report describes an AI-assisted drone survey for Mojave desert tortoises conducted between March 31 and May 15, 2024. The study area was composed of a series of 64 widely spaced 200m x 200m (4 ha) monitoring plots within the Boulder City Conservation Easement in Clark County, NV. Approximately 1,085 acres were subjected to low altitude photography using a drone during the period in which the animals were active aboveground. A computer vision model was used to detect tortoises and tortoise soil burrows in the acquired imagery.

- Six adult tortoises (Midline Carapace Length [MCL] >= 180 mm) were detected in the survey area, as well as one juvenile. Sixteen active or intact tortoise burrows were also detected.
- Tortoise density in the surveyed area was estimated to be 3.2/km^2 with a 95% confidence interval between 1.7 and 5.5 tortoises/km^2. Tortoise abundance in the Bounder City Conservation Easement as a whole was tentatively estimated to be 1107 with a 95% confidence interval between 591 and 1920, though this is based on a very small sample acreage.
- Tortoise populations are concentrated in the northeastern and southern portions of the easement.

Contents

List of Figures

List of Tables

1. Introduction

Small unmanned aerial vehicles (sUAS, or "drones") are becoming an important tool for wildlife biology, especially for population monitoring (e.g. Augustine and Burchfield 2022; Christie et al. 2016; Delplanque et al. 2021; Elmore et al. 2021; Huerta et al. 2020; Hyun et al. 2020; Inman et al. 2019; Jones et al. 2006; Linchant et al. 2018; Ramos et al. 2018; Watts et al. 2008; Zhou et al. 2021). Recent work conducted by Resi has shown that drone surveys can be an effective means of studying tortoise populations in the deserts of western North America (Bandy 2021, 2022; Bandy and Rognan 2022).

Between March 31 and May 15, 2024, Resi and Bio Logical, LLC partnered to conduct a drone survey within the Boulder City Conservation Easement (BCCE) in Clark County, NV (Figure 1.1). This work was conducted under contract to the Clark County Desert Conservation Program. The goal of the survey was to measure Mojave desert tortoise (*Gopherus agassizii*) occupancy within 70 established survey plots scattered throughout the project area. Charleston Shirley piloted the drone under contract to Bio Logical. Dan Roadhouse was Bio Logical's project manager. Matthew Bandy of Resi provided training, helped to oversee the fieldwork, and analyzed the data. Flights were conducted between 9 AM to 1 PM daily.

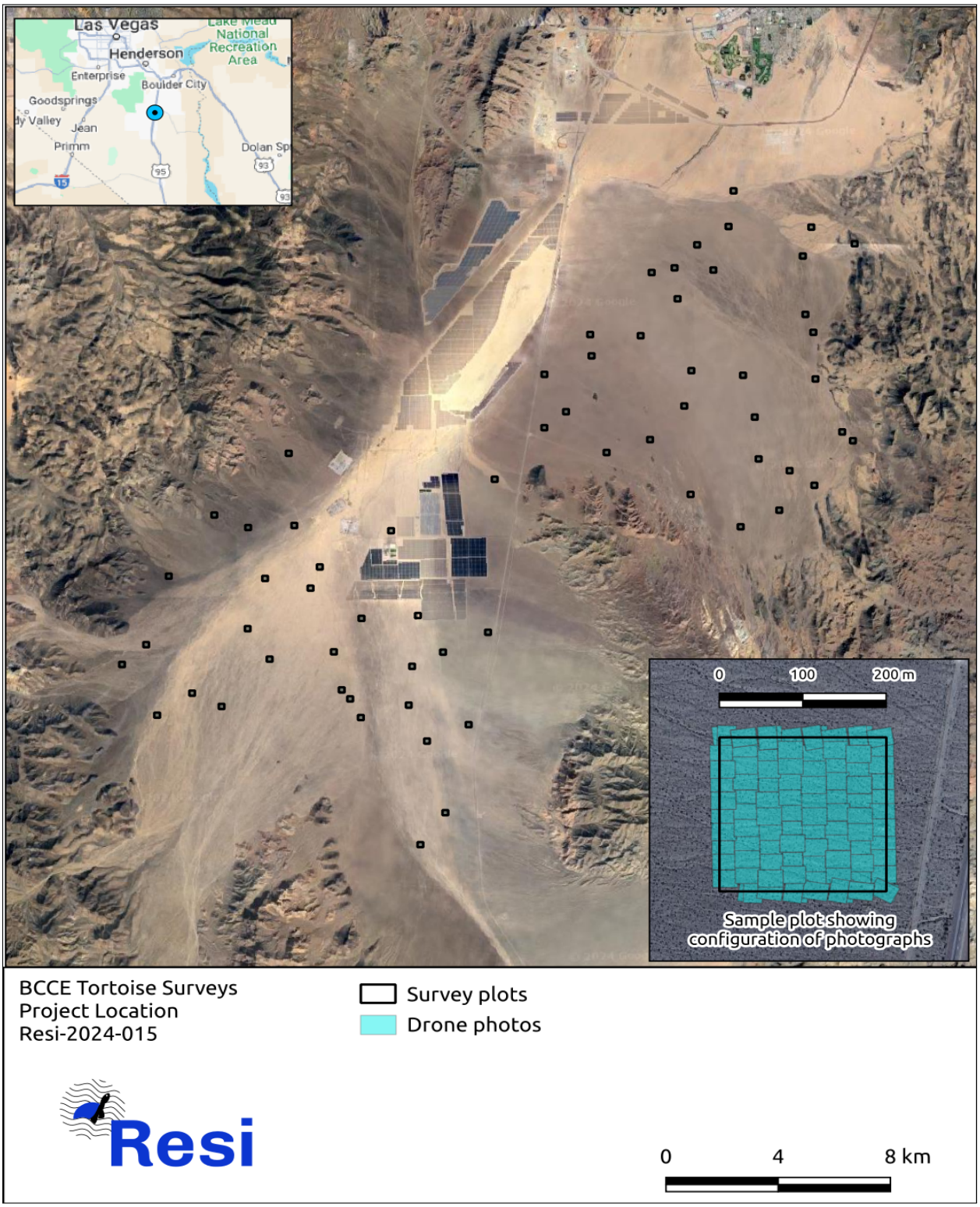

Figure 1.1. Project location map

2. Methods and Materials

The drone survey method, the use of trained convolutional neural networks for tortoise detection in drone photos, and Resi's bespoke implementation of distance sampling methods to generate density and abundance estimates from these detections is described in detail in Chapter 2 of Bandy (2022). The reader is referred to that document for a detailed treatment. The method will be described in only general terms below.

2.1. Drone Flights

The drone used was a DJI Mavic Enterprise mounted with the standard 20 megapixel camera. Flight planning and execution was performed using the Map Pilot Pro application. Charleston Shirley of Bio Logical planned the flights and piloted the aircraft. The target ground sample distance (GSD) was 5.5 mm. Previous studies (Bandy 2021; Bandy and Rognan 2022; Bandy 2022) have shown that 20 meters is the optimal flight elevation for the detection of adult Mojave desert tortoises using the selected hardware and software in the Mojave desert environment. All flights conducted as part of this survey were flown at 20 meters flight elevation. Terrain-following methods were employed to maintain a constant height above ground. This low flight elevation meant that the numerous transmission lines crossing the project area were significant impediments to flight safety. To avoid these dangers, no flights were performed within 500 feet of a transmission line or other hazardous facility such as a solar generation array.

Flights were planned to cover a total of 70 200x200 m (4 ha) established tortoise occupancy sample plots in conjunction with coordinated pedestrian surveys of the same plots. Drone surveys took place the day before the pedestrian surveys were performed in order to avoid any effect of pedestrian/tortoise interactions on animal behavior that might affect visibility of the animals to drone observation (Bandy 2023: 29). Flights were conducted Sunday through Thursday of each week. The schedule normally dictated six plot flights per day.

Each pedestrian plot measured 200x200 meters or 9.9 acres. Drone flights, however, typically photographed a somewhat larger area due to photo boundaries extending beyond the plot

footprint. The inset map on Figure 1.1 shows a typical photo configuration. The area photographed for a fully surveyed plot was approximately 12.1 acres, as show in Appendix A.

Six plots (plots 10, 35, 41, 51, 56, and 57) were eliminated from the sampling effort due proximity to a transmission line or solar array, and five additional plots were only partially flown (plots 37, 47, 50, 58, and 62; see Appendix A for photographed acreages by plot and day). The total drone survey sample was therefore composed of 59 complete plots and 5 partial plots. These were each flown three times over the course of three rounds of survey. The first round began on March 31, the second on April 14, and the third began on April 29 and ended on May 14 (Appendix A). Each round photographed a total area of approximately 748 acres, for a total survey effort of 2,244.3 acres photographed.

Tortoise survey flights were conducted between 9 AM and 1 PM. Previous studies have shown that tortoise visibility to drone photography varies dramatically by time of day (Bandy and Rognan 2022: 17-20; Bandy 2023: 14-16). In particular, in the afternoons tortoises tend to be located in their burrows or under the shade of vegetation, where they may be visible to pedestrian surveyors but are invisible from the air. In the mornings, by contrast, the animals are much more likely to be actively foraging or in motion and not under cover. Drone surveys conducted in the afternoons are therefore largely ineffective.

2.2. Computer Vision

Photographs were processed by a computer vision model trained by Resi using the PyTorch framework (Paszke et al. 2019), an open source environment for creating and training convolutional neural networks (CNNs). All drone photographs collected in the course of this project were processed by Resi's CNN models and tortoise detections were tabulated and geolocated. All detections received a final review by a human observer. MCL was determined by measuring the length of the carapace on the photograph in pixels, then multiplying this quantity by the GSD of the photograph (for this project, 5.5 mm).

2.3. Distance Analysis

Distance sampling is a family of statistical methods that use observations of the distance of detections from an observer to estimate density and abundance of a population (Buckland et al. 2001; Thomas et al. 2010; Miller et al. 2013, 2017). Resi has developed DroneDistance: a novel implementation of point distance sampling that treats drone photographs as

rectangular point samples. The DRONEDISTANCE R package was used to generate density and abundance estimates from raw tortoise detection data. The statistical methodology underpinning these calculations was first outlined in detail in Bandy (2022). That discussion is reproduced below.

2.3.1. The DRONEDISTANCE R package

DRONEDISTANCE is an R package developed by Resi for distance sampling and analysis of aerial photographic datasets. It is an entirely novel implementation of the distance sampling methodology and shares no code with DISTANCE 7.5 or its predecessors. Aerial photos are conceptualized as point samples that are truncated at the photo boundary. That is to say that each photograph is a rectangular point sample and the distance to detections is measured from the center of the photograph (i.e. the location of the drone at the instant the photograph was taken). The package accounts for photo distribution and overlap in its estimation of detection rates. Inputs to the package are spatial datasets describing photo boundaries and detection locations. The DRONEDISTANCE workflow and statistical methodology is outlined in the following sections.

2.3.2. Fitting the distance model $g(r)$

The first step is to fit a model describing the relationship between detection probability and distance from the center of the photograph. Photo data are read from *.csv* files with well-known text (WKT) polygons and points describing the boundary and center of each photograph measured in meters with a consistent coordinate system among all the photos (e.g., UTM coordinates from the same zone). Detection locations are read from a separate *.csv* with WKT points specifying detections. If an individual is detected more than once (e.g., in two intersecting photos), both detections are included in the *.csv*. However, one of the detections is identified as a duplicate in an additional column that gives F or FALSE for one of the detections and T or TRUE for the duplicate(s). The detections file must also include a column with unique identifiers for the photos in which they were detected, typically a globally unique identifier (GUID). Each unique identifier must have a corresponding entry in the photo polygons file.

The detection function is fit by maximum likelihood estimation, using Poisson regression of the number of detections as a function of the square of the distance from the center of the photograph. An offset term accounts for the area searched at each distance. The

model requires that each photograph be split into a large number of concentric rings (100 by default), and the area in each ring calculated and the number of detections tallied.

The probability of detection is assumed to decrease with distance from the center of the photograph as a half-normal probability density function (PDF), scaled so that $g(0) = 1$. The $g(0) = 1$ assumption is normally unrealistic, particularly when searching for cryptic taxa such as the desert tortoise, so it is scaled by g_0 in a subsequent step.

2.3.3. Estimation of g_r

The overall detection probability for individuals within a surveyed area is the integral of the distance function ($g(r)$,described above) over all the photographs with an adjustment for the areas of photo intersection. Exact evaluation of the integral and the adjustment for intersections would involve intricate bookkeeping, which is difficult to code, debug, and maintain. As an alternative, DRONEDISTANCE approximates the integral by generating a large number (default is 10,000) of random locations in the coverage area, calculating $g(r)$ for each location and taking the average. Locations that are in a single photograph would be assumed to have $g = g(r_{i,j})$, where $r_{i,j}$ is the distance between the location (i) and the center of photograph (j).

Locations (i) that are in the intersection of two photographs (j and k) are assigned a detection probability of

$$g = 1 - (1 - g(r_{i,j}))(1 - a \cdot g(r_{i,k}))$$

where a is a parameter that measures the degree of independence between observations in intersecting photographs. A value of $a = 0$ implies complete dependence, so that detection in one photograph implies a detection in the second photograph as well, while $a = 1$ implies complete independence between the observations. In practice, the detections are likely to have some degree of dependence, in which case the independence assumption will contribute to overestimation of g in the intersections, and the assumption of total dependence will contribute to slight underestimation of g in the intersections. The fraction of detection locations that are in three or more photos is normally small; and, as the number of intersecting photos increases, the degree of dependence among them increases.[1]

Thus, after accounting for dependence in the first two photos, each additional intersecting photo adds little to no independent information, and higher level terms in the estimation of

[1]For example, if there are 100 photos taken from slightly different angles, detections in photos from essentially the same locations will be very likely to have the same result.

g in intersections are ignored. That is, g is estimated as $1-(1-g_1)(1-ag_2)$ rather than $1-(1-g_1)(1-ag_2)...(1-a_ng_n)$.

2.3.4. Estimation of g_0

Detectability of individuals in the center of a photograph is estimated as $g_0 \sim beta(\alpha = x+0.5, \beta = n-x+0.5)$, where n is the total known individuals and x is an accurate count of whether the individuals would be detectable. This is the posterior distribution for the binomial p parameter, derived from a (non-informative) Jeffreys prior. These data must be generated by a separate survey effort typically involving observation of telemetered tortoises to monitor daily activity patterns during the survey period. Non-detection may be due to shelter that obscures the individual (e.g., burrow, vegetation), coloration, ground texture, or other factors. In the absence of data applicable to a specific survey effort, other means of estimating g_0 must be employed.

2.3.5. Determination of g_m

The quantity g_m refers to the probability that a tortoise present and visible in a photograph will be detected by the computer vision object detection system. In practice, this is the same as the recall value of the trained CNN model as determined by model validation procedures. This value is a property of the trained CNN itself and is not related to the distance from the center of the photograph or to visual impediments. It is therefore distinct from g_r and g_0.

2.3.6. A Partially Bayesian Solution for Estimating N

The posterior distribution of the number of individuals, N, is taken as

$$P(N = n \mid X, \hat{g}_{adj}) \propto P(X \mid N, \hat{g}_{adj})P(N = n)$$

where X is the observed number of individuals, $\hat{g}_{adj} = \hat{g}_r\hat{g}_0g_m$ is the estimated overall detection probability, and $P(N = n)$ is a suitable (non-informative) prior distribution for N. The betabinomial is perhaps the most natural prior for N, and it is used by default in the DRONEDISTANCE package (v. 2.0). However, this requires that a beta distribution can be fit to $\hat{g}$. If it cannot, then a binomial prior can be used, with the final posterior N distribution calculated as the average of the posterior N_i distributions conditioned on

independent, simulated $\hat{g}_i$ values from the product $\hat{g}_r \hat{g}_0 g_m$, with the three factors estimated or determined independently.

2.3.7. Estimate of Density and Abundance Within the Study Area

Finally, the tortoise density within the study area is estimated as $\widehat{D} = \frac{N}{A}$ where A is the area photographed. A is determined in a GIS environment by performing a vector dissolve operation on the photo polygons and measuring the area of the resulting survey area polygon. Abundance is then calculated as the product of $\widehat{D}$ and the total area of the project site.

3. Results and Evidence of the Results

Drone surveys for the desert tortoise were completed between 9 AM and 1 PM between March 31 and May 14, 2024. They resulted in the detection of six adult tortoises (Midline Carapace Length [MCL] >= 180 mm) and one juvenile (Figure 3.1).

3.1. Distance Analysis

Distance analysis was performed using the DroneDistance R package, described above. Since six detections is not adequate to fit a detection curve, a function was employed that was fitted using 233 drone/AI detections of adult-sized tortoise surrogates from a trial conducted in Clark County, NV in 2022 in an environment comparable to that of the study area (Figure 3.2). The trial is described by Bandy (2022).

3.1.1. Estimate g_0

The quantity g_0 refers to the percentage of tortoises that are aboveground and available for detection during the survey period. The best practice is to derive this quantity from observations of telemetered tortoises collected during the time frame of the drone survey and in a nearby location, as has been done in Resi's recent surveys in southeastern Utah (Bandy 2022; Bandy and Rognan 2022; Bandy 2023). Since no g_0 data were collected during the current project, the quantity was estimated using an alternate method, as described below.

	Drone g_0	Pedestrian g_0	Ratio
UT 2022	0.58	0.75	0.77
UT 2023	0.73	0.89	0.82
Mean			0.80

Table 3.1. Measured g_0 values for pedestrian and drone surveys

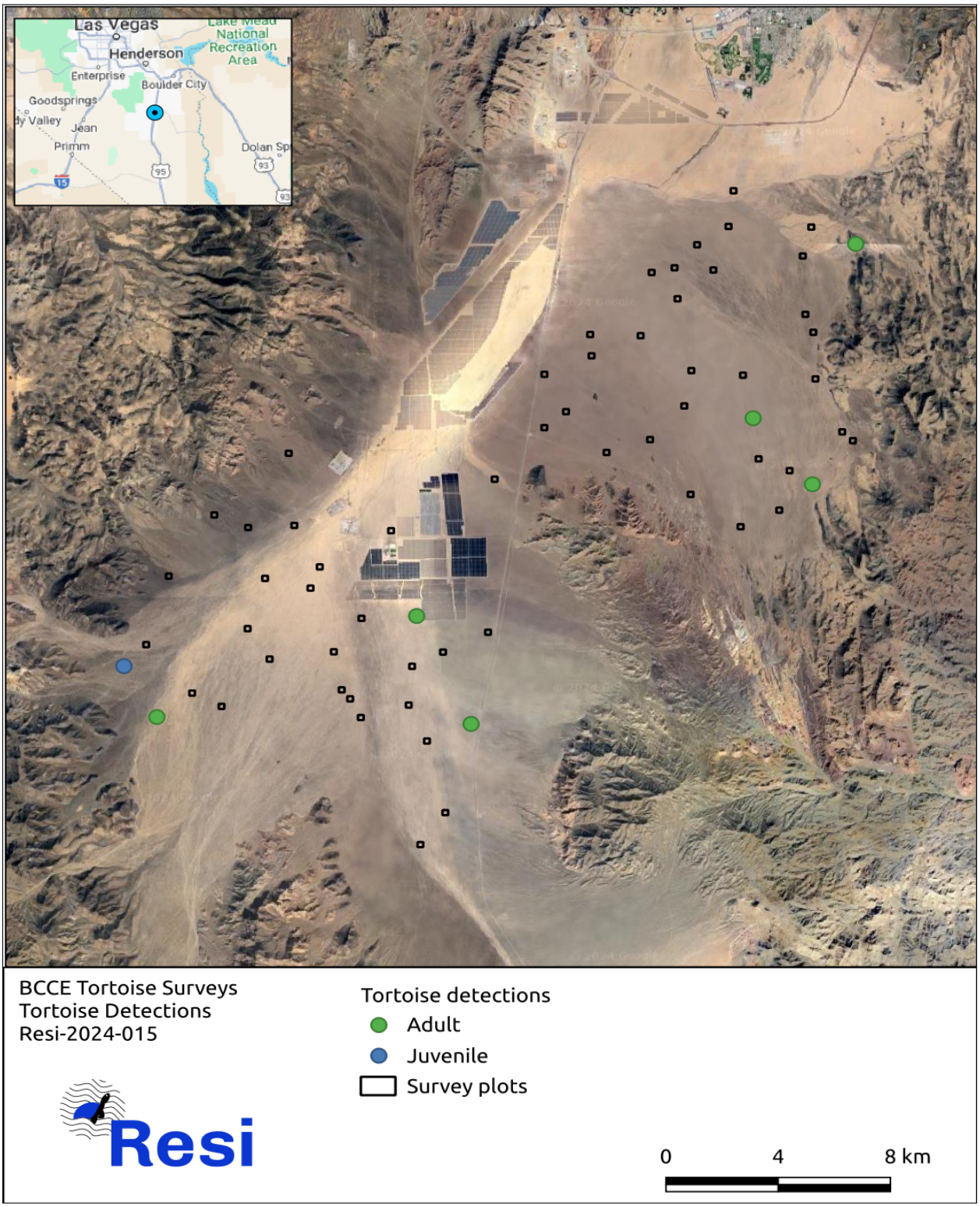

Figure 3.1. Tortoise detections

One method would be to calculate a g_0 value for drone observations from the value given by the USFWS protocol for pedestrian surveys. In general terms, g_0 for drone surveys is always lower than for pedestrian surveys. Resi has data from two projects for which good g_0 observations were collected in conjunction with the drone surveys (Bandy 2023, 2022). The ratio of drone g_0 values for the 9 AM to 1 PM timeframe to pedestrian g_0 values for the full day were 0.77 and 0.82, for a mean ratio of 0.80 (Table 3.1). Applying this correction to the value of pedestrian g_0 supplied by the pre-project survey protocol spreadsheet for the current area (0.73; U.S. Fish and Wildlife Service 2018: 8) yields a drone g_0 value of 0.58. This value was used in the distance analysis for the current project.

3.1.2. Combine $\hat{g}_0$, g_m and $\hat{g}_r$ into Estimated Overall Detection $\hat{g}$

The quantity g_r is estimated from the fitted distance model $g(r)$ and the drone photo polygons as described above and in Bandy (2022). It varies from one survey location to another due to the degree and configuration of photo overlap. In general, the higher the degree of photographic overlap in a dataset, the higher the overall detection probability will be. For the current study, mean $\hat{g}_r$ is estimated to be around 0.78 (Figure 3.3).

The quantity g_m is a property of Resi's trained CNN object detection model and is determined by evaluation of a separate validation sample segregated during model training. The validation sample employed in this study contained 118 randomly selected adult tortoise images. The model recall of this sample was 89.0% (105/118), so in this analysis $g_m = 0.89$. Again, this applies only to adult tortoises since data to confidently derive a g_m value for juveniles are not available.

The quantity $\hat{g}$ is an estimate of the tortoise detection probability throughout the entire aerial photographic dataset. It is calculated as the product of $\hat{g}_0$, g_m, and $\hat{g}_r$. For the current study, mean $\hat{g}$ is estimated to be 0.40 (Figure 3.4), meaning that we expect to detect approximately 40% of tortoises in the survey area using the drone/AI method.

3.1.3. Estimate Total Population N

N is the number of tortoises present in the photographed area (Figure 3.5). It is estimated from the number of detections and from $\hat{g}$ using the partially Bayesian method described above and in Bandy (2022: 9-10). For the current study, the total population within the photographed area is estimated to be 15 with a 95% confidence interval of 8-26.

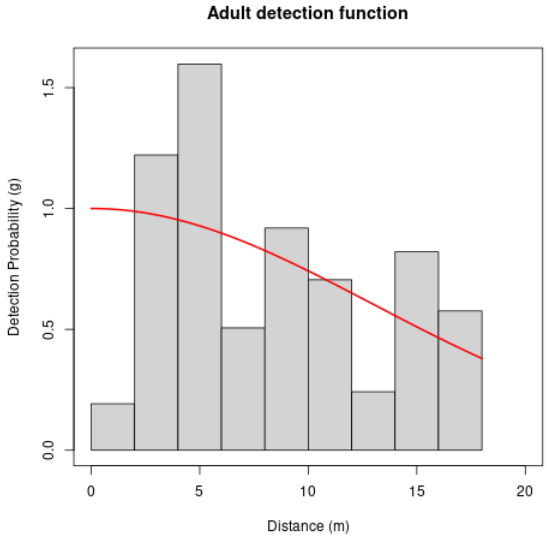

Figure 3.2. Half-normal distance model fitted to adult-sized tortoise surrogate detections ($I = 2.989e{-}3, AIC = 534.9$)

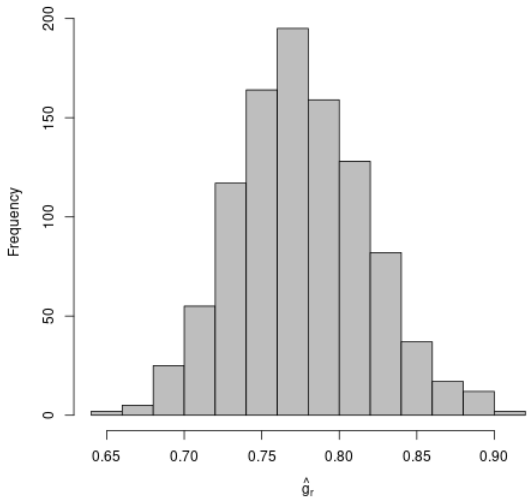

Figure 3.3. $\hat{g}_r$, adult tortoises

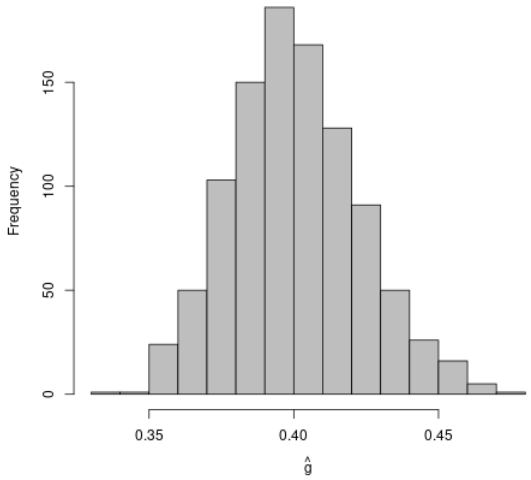

Figure 3.4. $\hat{g}$, adult tortoises

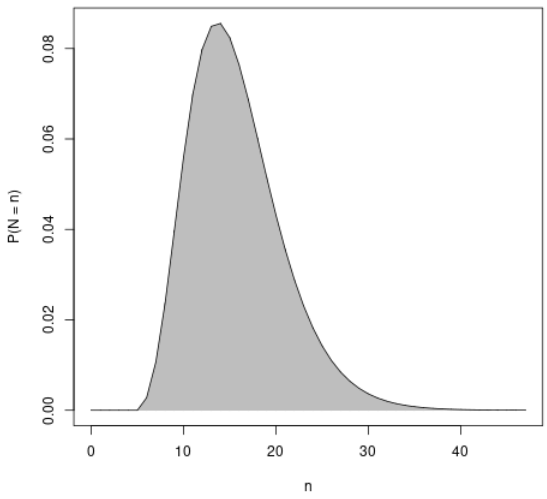

Figure 3.5. Estimated N, adult tortoises

3.1.4. Density and Abundance

Density is calculated by dividing N by the photographed area of each dataset. The photographed area is normally calculated in a GIS environment by performing a vector dissolve operation on the photo polygons and measuring the area of the resulting survey area polygon. However, this calculation was complicated by the fact that the Spring of 2024 was abnormally cold and aboveground tortoise activity did not begin until after the surveys had already started. Bio Logical pedestrian survey crews observed some tortoises in burrows as early as April 1, but no tortoises were seen active aboveground until April 19.[1] After that date tortoises were regularly observed in the open by pedestrian surveyors. This means that the first 16 out of the 34 total survey days took place when tortoises were not available for drone detection, and areas photographed during that interval should not be included in the total photographed area. A total of 1170.7 acres (4.74 km^2) were flown on or after April 19, so that number is used as the photographed area in this analysis.

The density of desert tortoises within the photographed area is estimated to be 3.2/km^2 with a 95% confidence interval between 1.7/km^2 and 5.5/km^2. Abundance is calculated by multiplying the density by the total project area (Table 3.2). The desert tortoise abundance within the 86,430-acre conservation easement is estimated to be 1107 with a 95% confidence interval of 591-1920. However, the surveyed area represents only about 1% of the whole project area, which reduces our confidence in the easement-wide population estimate.

N	km^2 Sampled	Density (N/km^2)	km^2 Total	Abundance
15 [8, 26]	4.74	3.2 [1.7, 5.5]	349.8	1107 [591, 1920]

Table 3.2. Density and abundance estimates with 95% confidence intervals.

3.2. Tortoise Burrows

While the primary goal of the drone surveys was to estimate density and abundance of tortoises, data on burrows was also collected. A CNN model was trained to detect burrows based on tagged images of 509 tortoise burrows from Resi's library. These were primarily Mojave desert tortoise burrow images collected from sites in California (n=194), Nevada (n=157), and Utah (n=55). Some images of Bolsón tortoise (*Gopherus flavomarginatus*) burrows were also included (n=103), as well as 251 landscape images that did not contain

[1] Incidentally, Mojave Max did not emerge until April 23, one of the latest emergences documented by the Mojave Max outreach program.

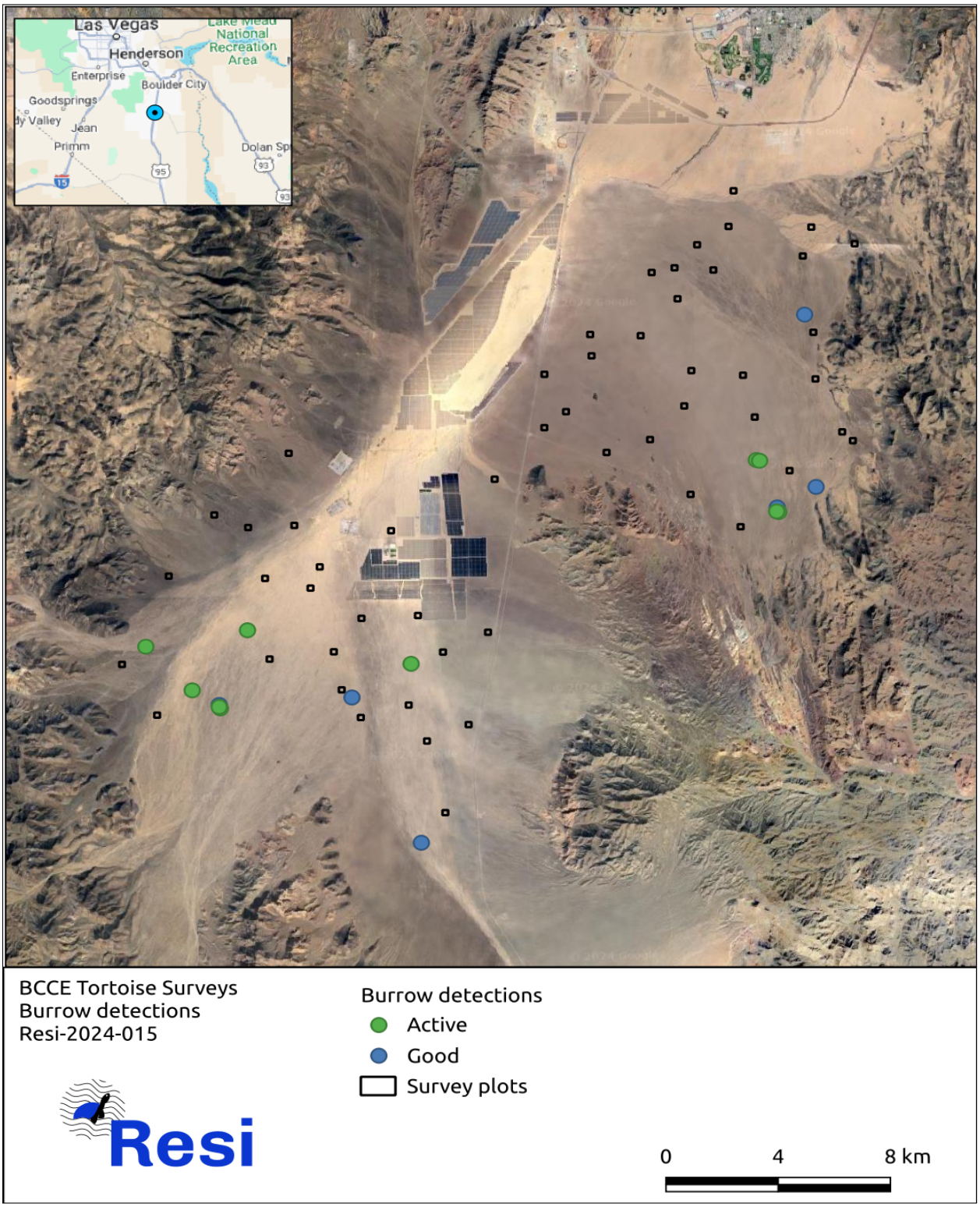

Figure 3.6. Burrow detections

any tortoise burrows. The trained model was effective, with a recall of approximately 0.82 and a precision of approximately 0.67 based on the validation dataset. As with tortoise detections, all burrow detections were reviewed in order to eliminate false positives and were classified as best as possible using the same schema employed in the USFWS pre-project survey protocol (U.S. Fish and Wildlife Service 2009).

A total of of 16 class 1 and 2 soil burrows were detected (Figure 3.6). The distribution of the burrows is consistent with tortoise detections in that burrows are concentrated in the northeastern and southern portions of the project area.

4. Conclusion and Recommendations

The drone/AI survey method was successful in detecting tortoises and burrows in the BCCE. The estimated population density of 3.2 tortoises/km^2 is somewhat higher than reported densities for this portion of the Mojave. For example, the nearby Ivanpah Valley Tortoise Conservation Area (TCA) had a density of 2.8 tortoises/km^2 in 2012 and 2.6 tortoises/km^2 in 2019, while the Eldorado Valley TCA had a density of 0.9 tortoises/km^2 in 2012 and 2.3 tortoises/km^2 in 2019 (Allison and McLuckie 2018; U.S. Fish and Wildlife Service 2020). However, tortoise populations are not evenly distributed within the project area. Rather, most tortoises appear to be concentrated within the southern and northeastern portions of the easement. Concentrations in these areas are relatively high, likely reflecting population augmentation actions.

This study has used distance sampling methods to estimate an easement-wide tortoise abundance of 1107 [591,1920]. However, this number should be viewed with skepticism. The sampled area represents only about 1% of the total land area of the BCCE, and any generalization from such a small sample is inherently weak. It is also worth noting that the survey methodology employed in this study was extremely inefficient. Flights were planned and timed to match the progress of the pedestrian survey, which limited survey coverage to approximately 70 acres per day. However, the drone/AI survey method is capable of much higher rates of coverage. Concurrently with the work reported here, Resi completed a survey of a large block of approximately 5,000 acres near Indian Springs, also in Clark County (Bandy 2024). This survey was completed in six days, at an average rate of about 850 acres per day. At that rate, the present study's 34 survey days could have produced data for as much as 30,000 acres—about a third of the acreage of the entire conservation easement, and about 13 times more area than was actually sampled. With a sample of that size, a reliable estimate of tortoise density and abundance across the entire study area could have been generated. It is strongly recommended that future applications of the drone/AI survey method employ sampling strategies that take advantage of the method's ability to very efficiently sample very large areas.

Literature Cited

Allison, L. J. and McLuckie, A. M. (2018). Population trends in Mojave desert tortoises (Gopherus agassizii). *Herpetological Conservation and Biology*, 13(2):433–452.

Augustine, J. K. and Burchfield, D. (2022). Evaluation of unmanned aerial vehicles for surveys of lek-mating grouse. *Wildlife Society Bulletin*, 46(4):e1333.

Bandy, M. (2021). Surveying for Desert Tortoises using Drones and Artificial Intelligence: A Pilot Study. Technical report 2021-001-01, Resi Solutions.

Bandy, M. (2022). A Method for Mojave Desert Tortoise Drone Surveys and a Controlled Field Test. Technical report 2022-001-02, Resi Solutions.

Bandy, M. (2023). Drone Surveys for the Mojave Desert Tortoise in Zones 2-5 of the Red Cliffs Desert Reserve. Technical report 2023-014-01, Resi Solutions.

Bandy, M. (2024). An AI-Assisted Drone Survey for Mojave Desert Tortoises within the Bonanza Solar Project Area, Clark County, NV. Technical report 2024-057-01, Resi Solutions.

Bandy, M. and Rognan, C. (2022). Drone and Pedestrian Desert Tortoise Surveys in Zone 6 of the Red Cliffs Desert Reserve. Technical report 2022-001-01, Resi Solutions.

Buckland, S. T., Anderson, D. R., Burnham, K. P., Laake, J. L., Borchers, D. L., and Thomas, L. (2001). *Introduction to distance sampling: estimating abundance of biological populations*. Oxford University Press.

Christie, K. S., Gilbert, S. L., Brown, C. L., Hatfield, M., and Hanson, L. (2016). Unmanned aircraft systems in wildlife research: current and future applications of a transformative technology. *Frontiers in Ecology and the Environment*, 14(5):241–251. _eprint: https://esajournals.onlinelibrary.wiley.com/doi/pdf/10.1002/fee.1281.

Delplanque, A., Foucher, S., Lejeune, P., Linchant, J., and ThÃ©au, J. (2021). Multispecies detection and identification of African mammals in aerial imagery using convolutional neural networks. *Remote Sensing in Ecology and Conservation*. Publisher: Wiley Online Library.

Elmore, J. A., Curran, M. F., Evans, K. O., Samiappan, S., Zhou, M., Pfeiffer, M. B., Blackwell, B. F., and Iglay, R. B. (2021). Evidence on the effectiveness of small unmanned aircraft systems (sUAS) as a survey tool for North American terrestrial, vertebrate animals: a systematic map protocol. *Environmental Evidence*, 10(1):1–6. Publisher: BMC.

Huerta, J. O., Henke, S. E., Perotto-Baldivieso, H. L., Wester, D. B., and Page, M. T. (2020). Ability of Observers to Detect Herpetofaunal Models Using Video from Unmanned Aerial Vehicles. *Herpetological Review*, 51(1):11–17.

Hyun, C.-U., Park, M., and Lee, W. Y. (2020). Remotely Piloted Aircraft System (RPAS)-Based Wildlife Detection: A Review and Case Studies in Maritime Antarctica. *Animals*, 10(2387):2387. Publisher: MDPI AG.

Inman, V. L., Kingsford, R. T., Chase, M. J., and Leggett, K. E. A. (2019). Drone-based effective counting and ageing of hippopotamus (Hippopotamus amphibius) in the Okavango Delta in Botswana. *bioRxiv*. Publisher: Cold Spring Harbor Laboratory _eprint: https://www.biorxiv.org/content/early/2019/07/01/689059.full.pdf.

Jones, G. P., Pearlstine, L. G., and Percival, H. F. (2006). An Assessment of Small Unmanned Aerial Vehicles for Wildlife Research. *Wildlife Society Bulletin*, 34(3):750–758. _eprint: https://onlinelibrary.wiley.com/doi/pdf/10.2193/0091-7648%282006%2934%5B750%3AAAOSUA%5D2.0.CO%3B2.

Linchant, J., Lhoest, S., Quevauvillers, S., Lejeune, P., Vermeulen, C., Ngabinzeke, J. S., Belanganayi, B. L., Delvingt, W., and BouchÃ©, P. (2018). UAS imagery reveals new survey opportunities for counting hippos. *PLoS ONE*, 13(11):e0206413. Publisher: Public Library of Science (PLoS).

Miller, D. L., Burt, M. L., Rexstad, E. A., and Thomas, L. (2013). Spatial models for distance sampling data: recent developments and future directions. *Methods in Ecology and Evolution*, 4(11):1001–1010. _eprint: https://besjournals.onlinelibrary.wiley.com/doi/pdf/10.1111/2041-210X.12105.

Miller, D. L., Rexstad, E., Thomas, L., Marshall, L., and Laake, J. L. (2017). Distance Sampling in R. *bioRxiv*. Publisher: Cold Spring Harbor Laboratory _eprint: https://www.biorxiv.org/content/early/2017/11/28/063891.full.pdf.

Paszke, A., Gross, S., Massa, F., Lerer, A., Bradbury, J., Chanan, G., Killeen, T., Lin, Z., Gimelshein, N., Antiga, L., Desmaison, A., Kopf, A., Yang, E., DeVito, Z., Raison, M., Tejani, A., Chilamkurthy, S., Steiner, B., Fang, L., Bai, J., and Chintala, S. (2019). PyTorch: An Imperative Style, High-Performance Deep Learning Library. In *Advances in Neural Information Processing Systems 32*, pages 8024–8035. Curran Associates, Inc.

Ramos, E. A., Ramos, E. A., Maloney, B., Maloney, B., Magnasco, M. O., Reiss, D., and Reiss, D. (2018). Bottlenose Dolphins and Antillean Manatees Respond to Small Multi-Rotor Unmanned Aerial Systems. *Frontiers in Marine Science*, 5. Publisher: Frontiers Media S.A.

Thomas, L., Buckland, S. T., Rexstad, E. A., Laake, J. L., Strindberg, S., Hedley, S. L., Bishop, J. R., Marques, T. A., and Burnham, K. P. (2010). Distance software: design and analysis of distance sampling surveys for estimating population size. *Journal of Applied Ecology*, 47(1):5–14. _eprint: https://besjournals.onlinelibrary.wiley.com/doi/pdf/10.1111/j.1365-2664.2009.01737.x.

U.S. Fish and Wildlife Service (2009). *Desert Tortoise (Mojave Population) Field Manual (Gopherus agassizii)*. Region 8, Sacramento, California.

U.S. Fish and Wildlife Service (2018). *Preparing for any Action that may Occur within the Range of the Mojave Desert Tortoise (Gopherus agassizii)*. Region 8, Sacramento, California.

U.S. Fish and Wildlife Service (2020). Range-Wide Monitoring of the Mojave Desert Tortoise (Gopherus Agassizii): 2019 Annual Reporting. Technical report, Desert Tortoise Recovery Office, Reno, Nevada.

Watts, A. C., Bowman, W. S., Abd-Elrahman, A. H., Mohamed, A., Wilkinson, B. E., Perry, J., Kaddoura, Y. O., and Lee, K. (2008). Unmanned Aircraft Systems (UASs) for Ecological Research and Natural-Resource Monitoring (Florida). *Ecological Restoration*, 26(1):13–14. _eprint: http://er.uwpress.org/content/26/1/13.full.pdf+html.

Zhou, M., Elmore, J. A., Samiappan, S., Evans, K. O., Pfeiffer, M. B., Blackwell, B. F., and Iglay, R. B. (2021). Improving Animal Monitoring Using Small Unmanned Aircraft Systems (sUAS) and Deep Learning Networks. *Sensors*, 21(5697):5697. Publisher: MDPI AG.

Appendix A.

Survey Effort by Plot and Date

Table A.1. Survey effort summary by plot and date

Round	Date	Plot	Photo count	Photographed acres
1	2024-03-31	01	88	12.1
1	2024-04-01	02	94	12.1
1	2024-03-31	05	88	12.1
1	2024-03-31	06	95	12.1
1	2024-03-31	08	86	11.7
1	2024-04-03	09	94	12.1
1	2024-04-03	11	94	12.1
1	2024-04-03	12	94	12.1
1	2024-04-03	13	94	12.1
1	2024-04-03	15	94	12.1
1	2024-04-01	17	94	12.1
1	2024-04-02	18	94	12.1
1	2024-04-02	19	94	12.1
1	2024-04-01	20	94	12.1
1	2024-04-02	21	88	12.1
1	2024-04-10	22	94	12.1
1	2024-04-02	23	94	12.1
1	2024-04-04	24	94	12.1
1	2024-04-03	25	94	12.1
1	2024-04-01	26	94	12.1
1	2024-04-02	27	94	12.1
1	2024-04-04	28	94	12.1

Table A.1. Survey effort summary by plot and date

Round	Date	Plot	Photo count	Photographed acres
1	2024-04-04	29	94	12.1
1	2024-04-01	30	94	12.1
1	2024-04-04	31	94	12.1
1	2024-04-01	32	98	12.1
1	2024-04-04	33	94	12.1
1	2024-04-10	34	94	12.1
1	2024-04-10	36	94	12.1
1	2024-04-04	37	22	3.0
1	2024-04-05	38	94	12.1
1	2024-04-02	39	94	12.1
1	2024-04-05	40	94	12.1
1	2024-04-05	43	99	12.1
1	2024-04-10	45	94	12.1
1	2024-04-05	46	94	12.1
1	2024-04-11	47	97	12.2
1	2024-04-11	48	59	7.1
1	2024-04-09	49	94	12.1
1	2024-04-05	50	64	7.8
1	2024-04-09	52	94	12.1
1	2024-04-11	53	94	12.1
1	2024-04-11	54	94	12.1
1	2024-04-09	55	94	12.1
1	2024-04-07	58	26	3.4
1	2024-04-08	59	94	12.1
1	2024-04-11	60	94	12.1
1	2024-04-07	61	94	12.1
1	2024-04-11	62	63	7.6
1	2024-04-08	63	94	12.1
1	2024-04-07	64	94	12.1
1	2024-04-08	65	94	12.1
1	2024-04-11	66	95	12.1
1	2024-04-07	68	94	12.1
1	2024-04-09	69	94	12.1

Table A.1. Survey effort summary by plot and date

Round	Date	Plot	Photo count	Photographed acres
1	2024-04-08	70	94	12.1
1	2024-04-08	71	88	12.1
1	2024-04-07	72	94	12.1
1	2024-04-09	73	94	12.1
1	2024-04-08	74	94	12.1
1	2024-04-07	75	94	12.1
1	2024-04-10	77	94	12.1
1	2024-04-10	79	94	12.1
1	2024-04-09	80	94	12.1
2	2024-04-14	01	94	12.1
2	2024-04-14	02	94	12.1
2	2024-04-14	05	94	12.1
2	2024-04-14	06	95	12.1
2	2024-04-14	08	97	12.2
2	2024-04-21	09	94	12.1
2	2024-04-21	11	94	12.1
2	2024-04-21	12	94	12.1
2	2024-04-21	13	94	12.1
2	2024-04-21	15	94	12.1
2	2024-04-15	17	94	12.1
2	2024-04-16	18	94	12.1
2	2024-04-16	19	94	12.1
2	2024-04-15	20	94	12.1
2	2024-04-16	21	94	12.1
2	2024-04-24	22	94	12.1
2	2024-04-16	23	94	12.1
2	2024-04-24	24	94	12.1
2	2024-04-21	25	94	12.1
2	2024-04-15	26	94	12.1
2	2024-04-16	27	94	12.1
2	2024-04-24	28	94	12.1
2	2024-04-24	29	94	12.1
2	2024-04-15	30	94	12.1

Table A.1. Survey effort summary by plot and date

Round	Date	Plot	Photo count	Photographed acres
2	2024-04-22	31	94	12.1
2	2024-04-15	32	98	12.1
2	2024-04-22	33	94	12.1
2	2024-04-24	34	94	12.1
2	2024-04-24	36	94	12.1
2	2024-04-22	37	22	3.0
2	2024-04-22	38	94	12.1
2	2024-04-16	39	94	12.1
2	2024-04-22	40	94	12.1
2	2024-04-17	43	99	12.1
2	2024-04-25	45	94	12.1
2	2024-04-22	46	94	12.1
2	2024-04-28	47	97	12.2
2	2024-04-28	48	59	7.1
2	2024-04-17	49	94	12.1
2	2024-04-17	50	65	7.9
2	2024-04-17	52	94	12.1
2	2024-04-28	53	94	12.1
2	2024-04-17	55	94	12.1
2	2024-04-18	58	26	3.4
2	2024-04-23	59	94	12.1
2	2024-04-28	60	94	12.1
2	2024-04-18	61	94	12.1
2	2024-04-28	62	63	7.6
2	2024-04-23	63	94	12.1
2	2024-04-18	64	94	12.1
2	2024-04-23	65	94	12.1
2	2024-04-28	66	95	12.1
2	2024-04-18	68	94	12.1
2	2024-04-25	69	94	12.1
2	2024-04-23	70	94	12.1
2	2024-04-23	71	94	12.1
2	2024-04-18	72	94	12.1

Table A.1. Survey effort summary by plot and date

Round	Date	Plot	Photo count	Photographed acres
2	2024-04-25	73	94	12.1
2	2024-04-23	74	94	12.1
2	2024-04-18	75	94	12.1
2	2024-04-25	77	94	12.1
2	2024-04-25	79	94	12.1
2	2024-04-25	80	94	12.1
3	2024-04-29	01	94	12.1
3	2024-04-29	02	94	12.1
3	2024-04-29	05	94	12.1
3	2024-04-29	06	95	12.1
3	2024-04-29	08	97	12.1
3	2024-05-01	09	94	12.1
3	2024-05-01	11	94	12.1
3	2024-05-01	12	94	12.1
3	2024-05-01	13	94	12.1
3	2024-05-01	15	94	12.1
3	2024-04-30	17	94	12.1
3	2024-05-05	18	94	12.1
3	2024-05-05	19	94	12.1
3	2024-04-30	20	94	12.1
3	2024-05-05	21	94	12.1
3	2024-05-07	22	94	12.1
3	2024-05-05	23	94	12.1
3	2024-05-06	24	94	12.1
3	2024-05-01	25	94	12.1
3	2024-04-30	26	94	12.1
3	2024-05-05	27	94	12.1
3	2024-05-06	28	94	12.1
3	2024-05-06	29	94	12.1
3	2024-04-30	30	94	12.1
3	2024-05-06	31	94	12.1
3	2024-04-30	32	98	12.1
3	2024-05-06	33	94	12.1

Table A.1. Survey effort summary by plot and date

Round	Date	Plot	Photo count	Photographed acres
3	2024-05-07	34	94	12.1
3	2024-05-07	36	94	12.1
3	2024-05-06	37	22	3.0
3	2024-05-07	38	94	12.1
3	2024-05-05	39	94	12.1
3	2024-05-07	40	94	12.1
3	2024-05-08	43	99	12.1
3	2024-05-15	45	94	12.1
3	2024-05-07	46	94	12.1
3	2024-05-08	47	97	12.2
3	2024-05-08	48	59	7.0
3	2024-05-08	49	94	12.1
3	2024-05-08	50	65	7.9
3	2024-05-08	52	94	12.1
3	2024-05-09	53	94	12.1
3	2024-05-09	54	94	12.1
3	2024-05-08	55	94	12.1
3	2024-05-12	58	26	3.4
3	2024-05-13	59	94	12.1
3	2024-05-09	60	94	12.1
3	2024-05-12	61	94	12.1
3	2024-05-09	62	65	7.8
3	2024-05-13	63	94	12.1
3	2024-05-12	64	94	12.1
3	2024-05-13	65	94	12.1
3	2024-05-09	66	95	12.1
3	2024-05-12	68	94	12.1
3	2024-05-14	69	94	12.1
3	2024-05-13	70	94	12.1
3	2024-05-13	71	94	12.1
3	2024-05-12	72	94	12.1
3	2024-05-14	73	94	12.1
3	2024-05-13	74	94	12.1

Table A.1. Survey effort summary by plot and date

Round	Date	Plot	Photo count	Photographed acres
3	2024-05-12	75	94	12.1
3	2024-05-14	77	94	12.1
3	2024-05-14	79	88	12.1
3	2024-05-14	80	94	12.1